Dual-Polarized FM Noise Radar

Garrett Zook*, Patrick M. McCormick*, Shannon D. Blunt*, Chris Allen*, John Jakabosky* †

**Radar Systems Lab, University of Kansas, Lawrence, KS, USA*
†Radar Division, Naval Research Laboratory, Washington, DC, USA

Keywords: Polarimetric radar, FM noise radar

Abstract

A technique denoted as pseudo-random optimized (PRO) FM has recently been experimentally demonstrated to facilitate a form of FM noise radar emission involving a unique, transmitter-compatible waveform for each pulse. Because the range sidelobes change each pulse, they are effectively suppressed when performing coherent integration (i.e. Doppler processing) over multiple pulses. Here, the PRO-FM scheme is incorporated into a dual-polarized arrangement, with independent waveforms emitted from each orthogonally polarized channel, as a means to suppress the cross-correlation effects that otherwise arise from simultaneous transmission on both channels. Experimental measurements demonstrate the efficacy of this high-dimensional emission.

1 Introduction

Random noise radar, where the waveform possesses randomly generated amplitude and phase to appear noise-like (e.g. [1-3]), has been well studied in the literature. The notion of FM noise radar, in which the waveform is constant amplitude with random frequency modulation, is less well-known and has previously been limited to analytical study [4]. Traditional noise radar is known to be inherently low probability of intercept (LPI) while tending to be limited to low-power, short-range applications due to noise-like amplitude modulation. In contrast, FM noise radar is not LPI but the constant-amplitude, spectrally well-contained nature of FM is consistent with the use of a saturated power amplifier, thus enabling high-power, long-range applications.

A physical realization of FM noise radar was recently demonstrated [5,6]. Denoted as pseudo-random optimized (PRO) FM, this scheme generates pulses (or CW segments) with waveforms that are initially random FM signals and subsequently shaped spectrally via an alternating projection process to possess a power spectral density (PSD) conforming to a desired template (to the degree possible). The Gaussian PSD is an attractive choice because it corresponds to an associated waveform autocorrelation that is likewise Gaussian and thus yields low range sidelobes relative to the time-bandwidth product [7]. When coherently combined over a coherent processing interval (CPI) of such pulses (or CW segments) the varying sidelobe structures over the CPI do not combine coherently, thereby providing further sidelobe suppression. The time-varying, high-dimensional nature of this physical emission scheme has also recently been shown to 1) facilitate in-band spectral notches for interference avoidance while mitigating much of the degradation that otherwise occurs and 2) enable a form of tandem-hopped radar/communication for spectrum sharing [8-11].

Here the high dimensionality of the FM noise radar structure is exploited to generate dual-polarized pulsed emissions of sufficient separability on receive (to within the limit of the antenna polarization isolation) that the orthogonally polarized channels can transmit simultaneously. It is demonstrated using both simulation and experimental measurements that coherent integration over a CPI of these dual-polarized waveforms realizes a low enough cross-correlation to adequately separate the co-polarized and cross-polarized receive components.

2 PRO-FM

Each PRO-FM pulse is first initialized with a random FM waveform. This initialization is accomplished by generating an N-length code of random samples drawn from a uniform distribution on $[-\pi,+\pi]$. Representing normalized instantaneous frequency values, these N samples are used to produce an initial random FM waveform via the polyphase-coded FM (PCFM) implementation [12].

For $s_{0,m}(t)$ the initial random FM waveform for the mth pulse, the desired PSD $|G(f)|^2$, and a desired pulse amplitude shape $u(t)$, the optimization is performed by alternating between the application of [5,6]

$$r_{k+1,m}(t) = \mathrm{F}^{-1}\left\{|G(f)|\exp\left(j\angle \mathrm{F}\left\{s_{k,m}(t)\right\}\right)\right\} \tag{1}$$

and

$$s_{k+1,m}(t) = u(t)\exp\left(j\angle r_{k+1,m}(t)\right) \tag{2}$$

for K iterations. The operations F and F^{-1} are the Fourier and inverse Fourier transforms, and $\angle(\bullet)$ extracts the phase of the argument. We shall use a Gaussian PSD and a pulse amplitude shape that is a constant over the pulsewidth T (on time interval $[0,T]$) and zero elsewhere. Note that since the optimization in (1) and (2) requires use of discretized versions of $|G(f)|$, $u(t)$, $r_{k,m}(t)$, and $p_{k,m}(t)$, it is necessary to "over-sample" these with respect to 3-dB bandwidth to ensure sufficient fidelity (i.e. to account for enough of the spectral roll-off region). If amplitude modulation (AM) is permitted,

this design approach has also been shown to facilitate a hybrid FM waveform that achieves ultra-low sidelobes [13].

The set of M waveforms designed in this manner possess unique sidelobe structures. When M is relatively small a "range sidelobe modulation" effect is known to occur [14,15] that can hinder clutter cancellation performance. However, as M increases the combination of the non-coherent sidelobes produces an incoherent averaging effect that yields reduced sidelobes for the CPI as a whole [6]. Appropriate design of mismatched filters on a per-pulse basis can also improve overall sidelobe suppression [6,16,17], though this option does not extend to dual-polarized operation due to the presence of the cross-polarized waveform response.

3 Dual-Polarized PRO-FM

Traditional noise radar has previously been used in polarimetric implementations [18-21] for low-power, short-range applications. It was also recently shown [22] that a polarimetric form of adaptive pulse compression (APC) can be applied on receive to separate the co-polarized and cross-polarized responses for arbitrary FM waveforms, though the computational cost of adaptive processing can be somewhat high. Here the high-dimensional benefits of noise radar are exploited via the PRO-FM construct to facilitate high-power, long-range operation of simultaneous dual-polarized emissions that, given a sufficiently high M to suppress the sidelobes, requires only matched filtering on receive.

The extension of PRO-FM [5,6] to dual-polarized operation involves the generation of a second independent random FM waveform initialization and subsequent alternating projection optimization for each pulse. Note that the independent random generation of each waveform pair establishes an average cross-correlation that is inversely proportional to N (which approximates the initial time-bandwidth product BT, for B the 3-dB bandwidth). The subsequent spectral shaping to reduce autocorrelation sidelobes also serves to decrease B, and is thus expected to degrade (i.e. increase) the degree of cross-correlation between the pair of waveforms since no effort is made to minimize cross-correlation aside from relying on the random initializations. Spectral shaping optimization that appropriately balances between autocorrelation and cross-correlation sidelobes remains a topic of ongoing investigation.

As an example, consider the generation of dual-polarized PRO FM waveforms that have a 3-dB bandwidth of B = 200 MHz and a pulsewidth of T = 1 μs. Denoting $s_{m,\mathrm{H}}(t)$ and $s_{m,\mathrm{V}}(t)$ as the m = 1, …, M waveforms to be emitted from the horizontally and vertically polarized channels, respectively, the associated autocorrelations $a_{m,\mathrm{H}}(\tau)$ and $a_{m,\mathrm{V}}(\tau)$ and cross-correlation $a_{m,\mathrm{X}}(\tau)$ can be computed.

For M = 5000 pulses, the root-mean-square (RMS) combination over each set of auto/cross-correlations provides a sense of the average sidelobe level in a given auto/cross-correlation response. Figure 1 illustrates these RMS results, where it is found that, on average, the autocorrelation sidelobe levels (a_{H} RMS and a_{V} RMS) reach a peak sidelobe level (PSL) of around −37 dB. The sidelobe level is markedly higher for the cross-correlation (a_{X} RMS), which has a PSL of about −25 dB. In other words, on average one can expect the cross-correlation to dominate the sidelobe response on a per-pulse basis.

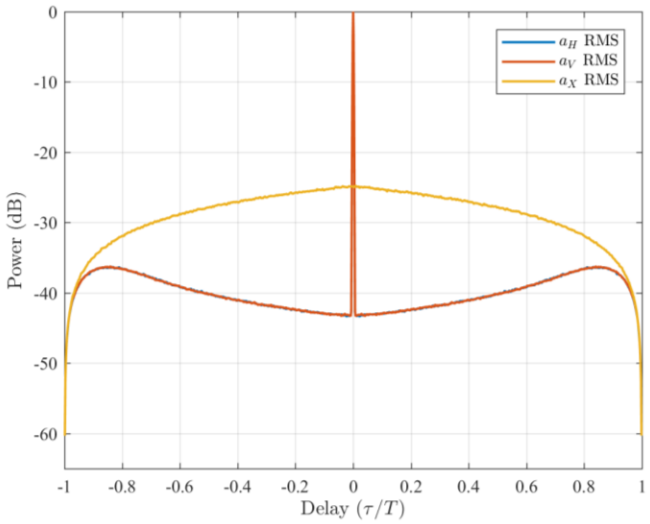

Fig. 1. RMS auto/cross-correlations for M = 5000 dual-polarized waveform pairs (note a_{H} RMS is virtually identical to a_{V} RMS)

When the M = 5000 auto/cross-correlations are coherently integrated such as would occur when performing Doppler processing, the responses in Figure 2 are obtained. Here it is observed that the autocorrelation responses (a_{H} and a_{V}) yield PSL values of around −69 dB and the cross-correlation (a_{X}) PSL is roughly −57 dB. These values are 32 dB lower than the RMS values for a single pulse from Fig. 1, which is 5 dB short of the 37 dB one would expect when combining 5000 incoherent pulses. This discrepancy is likely due to the spectral shaping which serves to constrain the available degrees of freedom one would expect from a spectrally white random instantiation.

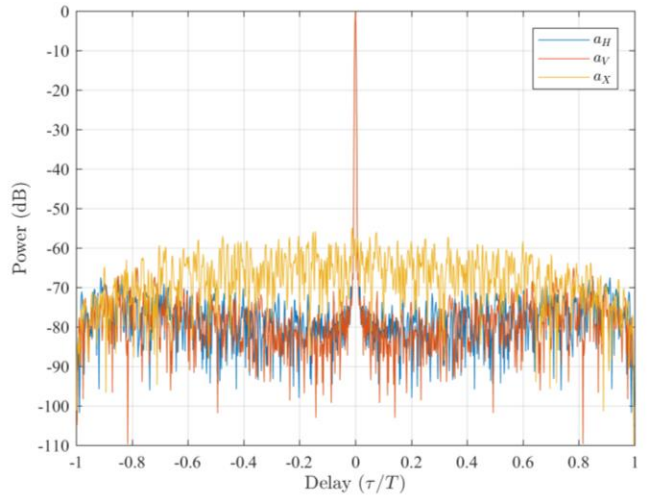

Fig. 2. Coherently integrated auto/cross-correlations for M = 5000 dual-polarized waveform pairs

If we alternatively consider M = 100 pulses, the auto/cross-correlations in Fig. 3 are obtained. As expected for a factor of 50 reduction in the number of independent pulses, a roughly 17 dB increase in the sidelobes is observed. In the next section we shall use this M = 5000 set of waveform pairs, in combination with pre-summing [23] as employed in some synthetic aperture radar (SAR) systems, to assess experimentally the separation of the dual-polarized components.

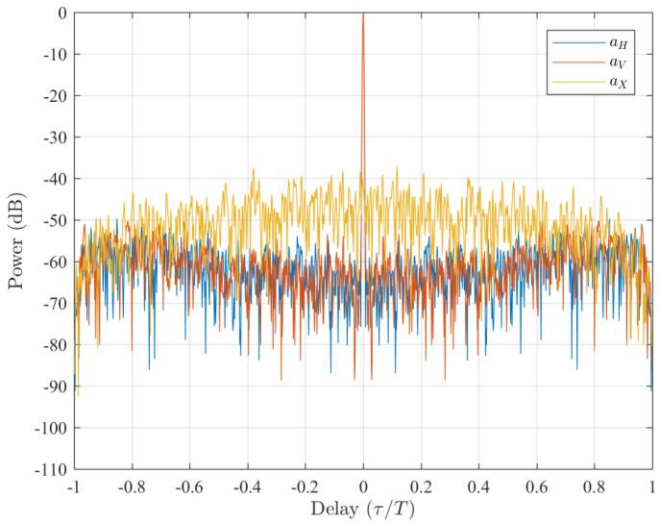

Fig. 3. Coherently integrated auto/cross-correlations for M = 100 dual-polarized waveform pairs

4 Free-Space Experimental Measurements

Using the dual-polarized waveform pairs from the previous section, free-space measurements were made from the roof of Nichols Hall on the University of Kansas campus. The target scene was the intersection of 23rd and Iowa streets at a radial range interval between 1050 m and 1250 m and consisted of multiple cars entering/leaving the intersection. Multiple campus buildings and treed areas were also within the field of view (see Figure 4).

Fig. 4. Field of view for free-space measurements.

The test setup is shown in Figure 5. The transmit and receive chains use separate offset horn-fed dish antennas with 22.5 dBi gain. The antennas have cross-polarization rejection of at least 25 dB and H/V port isolation of at least 20 dB. The transmit center frequency is 3.55 GHz. The wideband transmit amplifiers and receive low-noise amplifiers (LNAs) have 27 dB and 22 dB gain, respectively. The horizontal and vertical waveforms for each pulse were produced by two channels of a Tektronix AWG70002 waveform generator that has 10 bit resolution. The subsequent receive echoes were captured and digitized by a Tektronix DPO72304DX oscilloscope with 8 bit resolution.

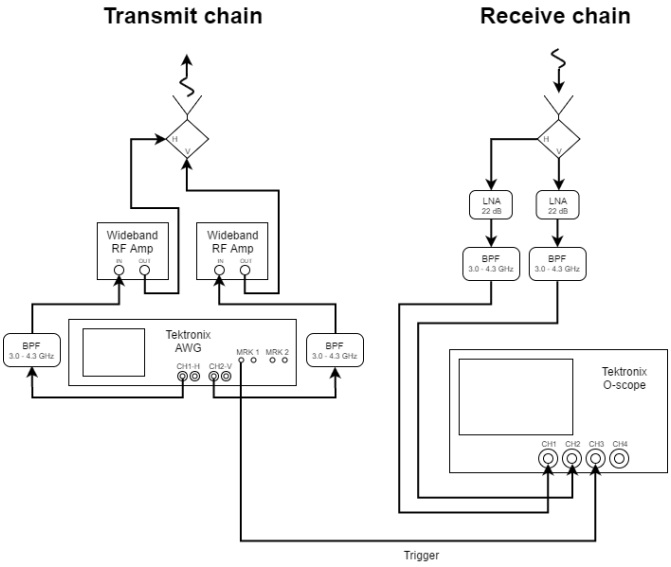

Fig. 5. Test setup for free-space measurements

This test setup is used to emit the M = 5000 PRO FM waveform pairs discussed in the previous section with a pulse repetition frequency (PRF) of 50 kHz (5% duty cycle). Thus the CPI comprises 0.1 seconds. Because this PRF is far higher than is necessary to measure the expected velocities of ground vehicles, the effective PRF can be reduced by pre-summing [23] a number of pulses prior to Doppler processing (but after pulse compression) which serves to low-pass filter the data in the Doppler domain.

While the pre-summing approach is well-known in SAR to reduce data handling/storage requirements [23], it has the additional benefit for these FM noise radar waveforms of providing greater dimensionality for incoherent sidelobe combining. For this case, the received echoes from the 5000 dual-polarized waveform pairs are first pulse compressed using their corresponding matched filters and then pre-summed by 50. Therefore, the effective PRF of 1 kHz, with an unambiguous velocity of 21.13 m/s. Doppler processing is then applied to the resulting 100 range profiles, thereby also reducing the computational load of the processing (especially clutter cancellation).

Figures 6-9 depict the HH, VV, and HV polarized responses from the target scene after clutter cancellation, which was implemented by simply projecting out the zero Doppler component. Multiple moving targets can be observed and the simultaneous illumination of both H and V channels enables direct comparison of the different responses without reducing the PRF to accommodate alternating illumination. It should

be noted that the vertically polarized receive channel was experiencing a sporadically faulty amplifier (hence the increased noise in the VV and HV responses) so these preliminary measurements will need to be repeated before firm conclusions can be drawn. That said, it is clear that usual information can be gleaned from the co-pol and cross-pol channels.

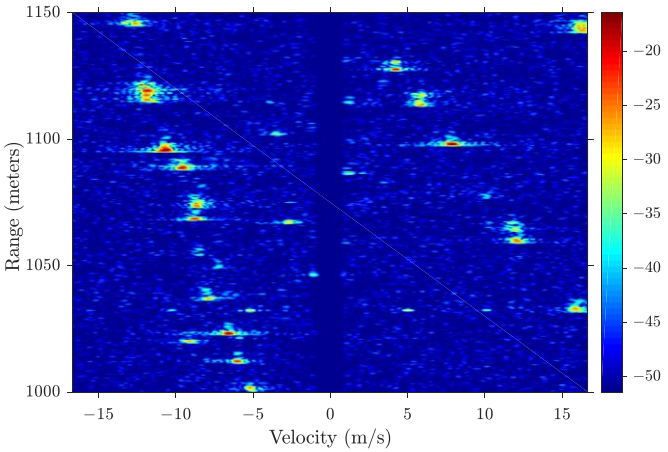

Fig. 7. HH range-Doppler response after clutter cancellation

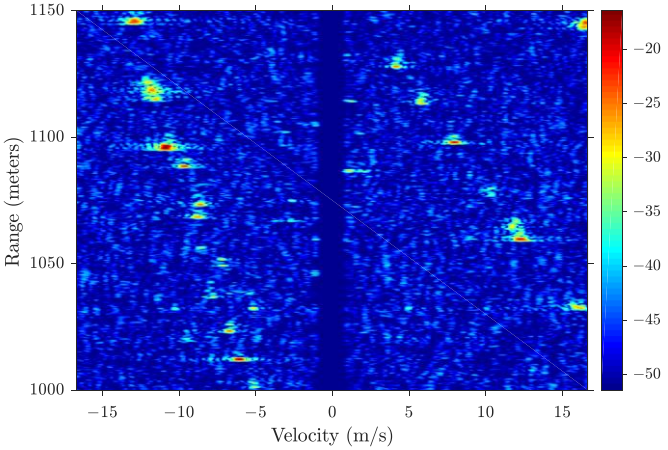

Fig. 8. VV range-Doppler response after clutter cancellation

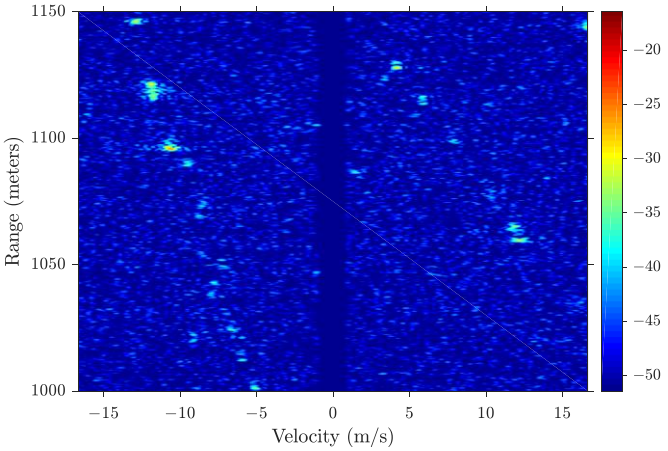

Fig. 9. HV range-Doppler response after clutter cancellation

5 Conclusions

Leveraging the pseudo-random optimized (PRO) FM noise radar emission, preliminary experimental measurements have demonstrated that dual-polarized FM noise radar can facilitate the emission of the horizontal and vertical channels simultaneous, thereby avoiding the need for alternating illumination. Such capability may also enhance performance for subsequent polarimetric processing [24,25]. Pre-summing, known to reduce data handling requirements for SAR, is also found to further enhance the benefit of incoherent sidelobe combining facilitated by the PRO FM scheme. Noting that the polarization isolation is a limiting factor on how well dual-polarized separation can be achieved, further measurements with greater isolation are needed to determine just how well FM noise radar can perform relative to the very good separation suggested by simulation.

Acknowledgements

This work was sponsored in part by the US Office of Naval Research under Contract #N00014-16-C-2029 and the US Naval Research Laboratory.

References

[1] B.M. Horton. “Noise-modulated distance measuring systems,” *Proc. IRE*, vol. 47, no. 5, pp. 821-828, May 1959.

[2] X. Xu, R.M. Narayanan. “Range sidelobe suppression technique for coherent ultra wide-band random noise radar imaging,” *IEEE Trans. Antennas & Propagation*, vol. 49, no. 12, pp. 1836-1842, Dec. 2001.

[3] M. Malanowski, K. Kulpa. “Detection of moving targets with continuous-wave noise radar: theory and measurements,” *IEEE Trans. Geoscience & Remote Science*, vol. 50, no. 9, pp. 3502-3509, Sept. 2012.

[4] S.R.J. Axelsson. “Noise radar using random phase and frequency modulation,” *IEEE Trans. Geoscience & Remote Sensing*, vol. 42, no. 11, pp. 2370-2384, Nov. 2004.

[5] J. Jakabosky, S.D. Blunt, B. Himed. "Waveform design and receive processing for nonrecurrent nonlinear FMCW radar," *IEEE Intl. Radar Conf.*, Washington, DC, USA, May 2015.

[6] J. Jakabosky, S.D. Blunt, B. Himed. "Spectral-shape optimized FM noise radar for pulse agility," *IEEE Radar Conf.*, Philadelphia, PA, USA, May 2016.

[7] J.A. Johnston and A.C. Fairhead, “Waveform design and Doppler sensitivity analysis for nonlinear FM chirp pulses,” *IEE Proc. Communications, Radar & Signal Processing*, vol. 133, no. 2, pp. 163-175, Apr. 1986.

[8] J. Jakabosky, S.D. Blunt, A. Martone. "Incorporating hopped spectral gaps into nonrecurrent nonlinear FMCW radar emissions," *IEEE Intl. Workshop on Computational Advances in Multi-Sensor Adaptive Processing*, Cancun, Mexico, Dec. 2015.

[9] J. Jakabosky, B. Ravenscroft, S.D. Blunt, A. Martone. "Gapped spectrum shaping for tandem-hopped

radar/communications & cognitive sensing," *IEEE Radar Conf.*, Philadelphia, PA, USA, May 2016.

[10] B. Ravenscroft, P.M. McCormick, S.D. Blunt, J. Jakabosky, J.G. Metcalf. "Tandem-hopped OFDM communications in spectral gaps of FM noise radar," *IEEE Radar Conference*, Seattle, WA, USA, May 2017.

[11] B. Ravenscroft, S.D. Blunt, C. Allen, A. Martone. "Analysis of spectral notching in FM noise radar using measured interference," *IET Intl. Radar Conf.*, Belfast, UK, Oct. 2017.

[12] S.D. Blunt, M. Cook, J. Jakabosky, J. de Graaf, E. Perrins. "Polyphase-coded FM (PCFM) radar waveforms, part I: implementation," *IEEE Trans. Aerospace & Electronic Systems*, vol. 50, no. 3, pp. 2218-2229, July 2014.

[13] J. Jakabosky, S.D. Blunt, and T. Higgins. "Ultra-low sidelobe waveform design via spectral shaping and LINC transmit architecture," *IEEE Intl. Radar Conf.*, Washington, DC, USA, May 2015.

[14] S. Blunt, M. Cook, J. Stiles. "Embedding information into radar emissions via waveform implementation," *Intl. Waveform Diversity & Design Conf.*, Niagara Falls, Canada, Aug. 2010.

[15] C. Sahin, J. Metcalf, and S. Blunt. "Mathematical characterization of range sidelobe modulation," *IET Intl. Radar Conf.*, Belfast, UK, Oct. 2017.

[16] A. O'Connor, J. Kantor, and J. Jakabosky. "Joint equalization filters that mitigate waveform-diversity modulation of clutter," *IEEE Radar Conf.*, Philadelphia, PA, USA, May 2016.

[17] C. Sahin, J. Metcalf, and S. Blunt. "Filter design to address range sidelobe modulation in transmit-encoded radar-embedded communications," *IEEE Radar Conf.*, Seattle, WA, USA, May 2017.

[18] Y. Xu, R.M. Narayanan, X. Xu, J.O. Curtis. "Polarimetric processing of coherent random noise radar for buried object detection," *IEEE Trans. Geoscience & Remote Sensing*, vol. 39, no. 3, pp. 467-478, Mar. 2001.

[19] R.M. Narayanan, C. Kumru. "Implementation of fully polarimetric random noise radar," *IEEE Antennas & Propagation Letters*, vol. 4, no. 1, pp. 125-128, June 2005.

[20] L. Maslikowski, K. Kulpa, D. Glushko, F. Yanovsky. "Atmospheric precipitation sensing with a short-range C-band noise radar," *Intl. Radar Symp.*, Dresden, Germany, June 2013.

[21] A. Stove, G. Galati, G. Pavan, F. De Palo, K. Lukin, K. Kulpa, J.S. Kulpa, L. Maslikowski. "The NATO SET-184 noise radar trials," *Intl. Radar Symp.*, Krakow, Poland, May 2016.

[22] P. McCormick, J. Jakabosky, S.D. Blunt, C. Allen, B. Himed. "Joint polarization/waveform design and adaptive receive processing," *IEEE Intl. Radar Conf.*, Washington, DC, USA, May 2015.

[23] W.M. Brown, G.G. Houser, R.E. Jenkins. "Synthetic aperture processing with limited storage and presumming," *IEEE Trans. Aerospace and Electronic Systems*, vol. AES-9, no. 2, pp. 166-176, Mar. 1973.

[24] D.L. Evans, T.G. Farr, J.J. van Zyl, and H.A. Zebker. "Radar polarimetry: analysis tools and applications," *IEEE Trans. Geoscience & Remote Sensing*, vol. 26, no. 6, pp. 774-789, Nov. 1988.

[25] R. Touzi, S. Goze, T. Le Toan, A. Lopes, and E. Mougin. "Polarimetric discriminators for SAR images," *IEEE Trans. Geoscience & Remote Sensing*, vol. 30, no. 5, pp. 973-980, Sept. 1992.